International Journal of Modern Manufacturing Technologies
ISSN 2067–3604, Vol. XIV, No. 3 / 2022
https://doi.org/ 10.54684/ijmmt.2022.14.3.124

MATHEMATICAL AND NUMERICAL SIMULATION OF THE THERMALLY HARDENED COATED MACHINE SURFACES

Salam J. Bash AlMaliki

Al-Iraqia University, College of Engineering, Baghdad, Iraq

Corresponding author: Salam J. Bash AlMaliki, salambash2000@yahoo.com

Abstract: The productivity of manufacturing activities is highly dependent on the quality of the processing machines and the readiness of their parts at all work times. The cutting tools are among these crucial parts for many manufacturing processes and hence their outer surfaces need continuous maintenance processes such as thermal hardening and coating. The physical and thermal properties of these outer surfaces are mathematically and numerically analyzed by the application of Ohm`s and Kirchhoff`s laws during the thermal hardening process to determine the best operation schemes and governing variables that may produce the highest performance and improve the quality of these machines` moving parts. The improvement of this maintenance process via the inclusion of the Nano-materials into the coating surfaces of the understudy parts is one of the tentative outcomes of these analyses. The results reflect the high role of the usage of inline cooling systems for the removal of heat, and that the maximum temperature in the contact area of the deformation region and corresponding processing speed, have a high share in the decision of the exterior layer`s material for the hardening work tool to develop into the critical state of shift instability.

Keywords: ANN, cooling process, hardening, mathematical model.

1. INTRODUCTION

Good selection of the control scheme of machine tools hardening process is one of the influential factors for the achievement of the desired results that suit the operational requirements and environment, through the identification and manipulation of the various variables that interfere with the rapid quench of heated steel or metal alloys to the temperature of austenitization, that varies according to their content of carbon, which turns them to the martensite phase (Blankart et al., 2021). Initially, the mechanisms of the austenization process are sophisticated due to its occurrence from diverse primary microstructures, like the cold recrystallized ferrite, tempered martensite, or a mix of cementite or pearlite and ferrite, in addition, alloying elements apply their impact in several ways at diverse stages of conversion (Weia et al., 2013). These transformations were tracked by many researchers in an attempt to specify the most effective variables and operation conditions, and some of these researchers used the thermal analysis and the Artificial Neural Network ANN procedure rather than the mathematical modeling, as more precise and direct means that may deal with the very three dimensional 3D details of the problem (Tarchoun et al., 2020, Farrahi and Sistaninia, 2009, Tan and Zhou, 2013, Hung et al., 2018). These models and their attributed validations indicated that the suggested numerical models can determine a reliable and precise hardened surface features approximation under capricious heating parameters and scanning forms. The anticipated model affords, in addition, an applicable foundation for a detailed analysis of the effects of the scanning form design constraints on the specifications of the hardened zone. However, many complications were documented as the major limitations of the use of the thermal analysis, such as the complexities of heat removal from the adjacent faces of the moving instrumental parts, and the shift of negative stability of the surfaces of the various coating materials, and hence favorite the mathematical modeling approach that adapts criterial equations for the determination of the boundary conditions on the understudy surfaces, instead (Jos ́e Manuel et al., 2017, Makarova et al., 2016).

This research aims to design an outline frame for a mathematical model to explain, evaluate, and manage the nanostructure outer surfaces of the coating constituents as a consequential result of the thermal hardening method, given the critical phase of the negative stability`s lowest temperature for the working machine part. The field experimental works are made in the Baghdad central industrial complex; Kasra and Atash east north Baghdad, which is considered the biggest private sector industrial activity in the capital of Iraq.

2. THEORETICAL ANALYSIS

Kirchhoff's laws for the flow of current through electrical circuits and its distribution across the nodes as illustrated in Figure 1, would be the base for the build of a generalized equivalent thermal pattern for the modeling of the heat transportations during the various steps of the hardening process through the multiple layers of the in contact machine`s moving parts. The simpler identification of this law is that the total currents entering and exiting a certain node are equal and that the energy is conserved inside the whole loop or circuit. The Ohm`s law (Figure 1b) would support the simulation of thermal notations by their equivalent electrical ones to suit the Kirchhoff`s approach, where the thermal resistance is represented by its reciprocal; thermal conductivity K and consequently the nodal notations would be Kij, also temperatures Ti would replace the voltage to represent the nodal temperatures in the equivalent circuit while the current through nodes would be replaced by the heat flow Qi to achieve the goal of simulating the heat removing system.

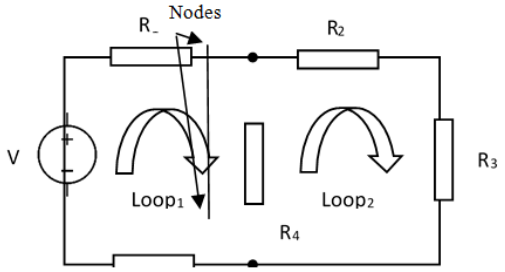

(a)

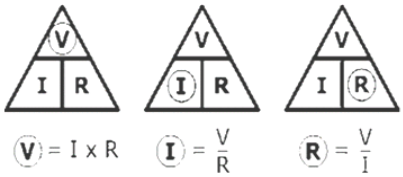

(b)

Fig. 1 schematic illustrations for the Kirchhoff`s law (a) and Ohm`s law (b) (Charles et al., 2012)

Based on the two mentioned laws, the thermos-physical properties of the hardening process for the surfaces of contact of the work machines materials can be demonstrated by the generalized n-nodes equivalent heat balance formula as follows:

$$Kn\,Tn = Qn \tag{1}$$

With the assumption of the adiabatic process, the working material`s highest temperature T_{max} that can be expected at the upper coating surface is determined as follows:

$$T_{max} = \pi r^2 = T_i = \pi r^2 + \frac{Q_{vic}}{K} \tag{2}$$

where: T_i stands for the initial temperature of the surface coating material, and Q_{vic} stands for heat flow from the high-speed capacity transmitter that spreads orthogonally to the vector of speed $_v$.

As the customization of the equivalent thermal approach for the demonstration of the heat dissipation process may be thought of as a special case of the finite-difference method, then the accuracy of the determined temperatures at each of the various nodes of the scheme is essentially attributed to the appropriateness of mathematical formulation for the conductivity/ resistance in the thermal circuit. The material`s bulk thermal resistance R_{mb} is calculated as follows:

$$R_{mb} = \frac{4h_n}{\pi K L^2{}_{con}} \tag{3}$$

where: L_{con} stands for the length of the contact face, and h_n stands for the thickness of the exterior coating side that is heated thru the thermal hardening process (Figure 2).

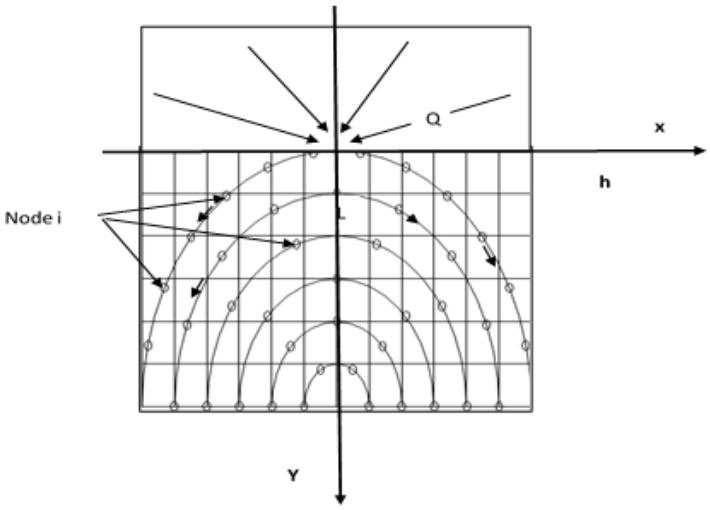

Fig. 2. A schematic of heat distribution in the contact area of the work tool material

The validity of the resulted model is tested by the comparison with the model of the ANN approach on the precision. The ANN consists of three layers; the inputs layer, the hidden layer, and the outputs layer, that linked to each other by weights and the preference between which is related to the Mean Square error MSE. The training of ANN through the backpropagation algorithm should pass three stages; the forward stage, the back pass stage, and the weights update stage (Mathioulakis et al., 2018). The input signals access each node of the hidden layer during the forward stage. The activation value for each of these nodes is to be calculated to be sent to the nodes of the outputs layer where the activation values are to be calculated there to form the network`s response for the given inputs. During the training stage, each node of the outputs layer does compare its calculated activation value with the actual value to determine the error value for that node, upon which, the coefficient of error correction δk is to be determined to distribute the error for all nodes in the outputs layer, and also that coefficient is used to update weights in the output and hidden layers. Similar to that, the coefficient of error correction in the nodes of the hidden layer δj is to be determined to update weighs in the hidden and inputs layers. The all-layers weights are instantaneously fitted according to the following steps (Yuehui et al., 2005, Bogdan and Stefan, 2014):

1. Set the values of primary weight.
2. Each node of the input layer receives the input signal and delivers it to all nodes in the hidden layer.
3. Nodes weighted input signal values in the hidden layer are summed as follows:

$$sh_i = \frac{2}{(1+ e^{-\sum_i x_i w_{ij}})} - 1 \quad (4)$$

where: w stands for the weight between layers, and x_i stands for the inputs.

4. The activation function is used to calculate the hidden layer`s outputs and send the activation values to all nodes in the outputs layer.
5. Nodes weighted input signal values of the in the output layer are summed as follows:

$$so_k = \frac{2}{(1+ e^{-\sum_j sh_j w_{jk}})} - 1 \quad (5)$$

6. The output node`s error is determined as the difference between the node`s output so_k (activation value) and the real value r_k, as follows:

$$OE_k = r_k - so_k \quad (6)$$

Then, the error δ_k is calculated according to the following formula:

$$\delta_k = OE_k \,.\, f(v) \quad (7)$$

Where $f(v)$ refers to the logistic function for the non-linear output nodes.

The variation in the errors Δw_{jk} is calculated as follows:

$$\Delta w_{jk} = \alpha \,.\, \delta_k \,.\, sh_j \quad (8)$$

While for the hidden layer it is as follows:

$$\Delta v_{ij} = \alpha . \delta_i . x_i \quad (9)$$

where: α is a constant.

7. The node weights in the outputs layer are consequently updated according to the formula:

$$w_{jk} \text{ (new)} = w_{jk} \text{ (old)} + \Delta w_{jk} \quad (10)$$

And for these in the hidden layer as follows:

$$v_{ij} \text{ (new)} = v_{ij} \text{ (old)} + \Delta v_{ij} \quad (11)$$

8. The system continues updating its weights; learning and training, to the extent of the finest weights that allow the resolve of the besieged yields.

3. RESULTS AND DISCUSSIONS

The thermal conductivity of the common coating materials that are used in this study are tabulated in table 1, which shows the decrease of this property in the Aluminium Oxide Al_2O_3 with the increase of operation temperature, hence this material is discarded from the experimental sets.

Table 1. The thermal conductivity of the common coating materials at various temperatures (Samani et al., 2015)

Coating material / property	Tin	TiCN	Al_2O_3
Thermal conductivity (W/m. C)	20(40 C)	26(25 C)	33(50 C)
	21(100 C)	27(100C)	28(90 C)
	22(300 C)	28(300 C)	19(300 C)
	23.5(500 C)	30(500 C)	13(500 C)
	26(1,000 C)	33(1,000 C)	7(1,000 C)
	27(1,300 C)	35(1,300 C)	7(1,300 C)

The general form of the machine indenting part`s volumetric thermal resistance is determined via the laboratory and field (industrial complex of Baghdad) experimental operations data and the substitution of

equation 3 in the following form to resolve the matrix and reach the general model, via the use of equation (2).

$$R_{om} = \frac{h_e}{K\, A_{tn}} \tag{12}$$

where: h_e, K, and A_{tn} are the altitude, thermal conductivity, and the heat transmission area of the work tool part, respectively.

The application of equation (12) determines the resistance at each joint/node, and this, in turn, facilitates the modeling of the mathematical form of the equivalent heat arrangement`s thermal resistances that describe the thermal hardening process of the contact surfaces in the work machine that states the importance of the appropriate flow of cooling media *m* to result in the necessary turbulent pattern for the continuous lubricant or coolant medium to overcome the Rapid change of the material's temperature in the boundary layer of the work part and on the surface of the indenter takes place due to the supply of heat constriction *qi* through joint thermal resistances. This is demonstrated by the relation:

$$m > \frac{R_e .\mu. A}{d1-d2} \tag{13}$$

where: *Re* is the Reynolds number at the turbulent flow pattern of the appropriate lubricating-cooling technological means; μ is fluid viscosity; A is the cross-section area of the turbulence stimulator channel in the work tool configuration; d_2 is the tool`s cage inside diameter; $d_1$ is the turbulence stimulating pipe`s outside diameter.

Based on the analytical research of the thermal physics of the trimming hardening processing of the machine parts' surfaces the classification of the work tool's heat removal system was created and based on numerical and physical simulation of processes that take place in the contact area, with the help of represented mathematical models the effective variants of their building were determined. These variants make it possible to implement the material Nanostructuring of the surface coating. It was determined that the material Nanostructuring of the parts of the surface coating during the trimming hardening processing using the criteria of plastic structure formation and processing rate is most effective when the work tool with the in-line cooling heat removal system of the hollow indenter is used by the lubricating - cooling technological environments under pressure.

The same field experimental data were dealt with via the use of the ANN analysis to determine the model that best simulates the hardening process and the nodal heat variations. The ANN approach by a single-step flow of the time series is tracked to result in the optimal estimate. The three-layered intended network; inputs, hidden, and output, are qualified reliant on the logistic function and the sigmoid function, through 1500 attempts in maximum or the accomplishment of the training settings. The hidden layer entails 25 nodes, whereas the outputs layer has a single node denoted by the variable x_t. The ANN precision of the training step is confirmed and found high as it almost indicates thorough equity to the field data as illustrated in Figure 3.

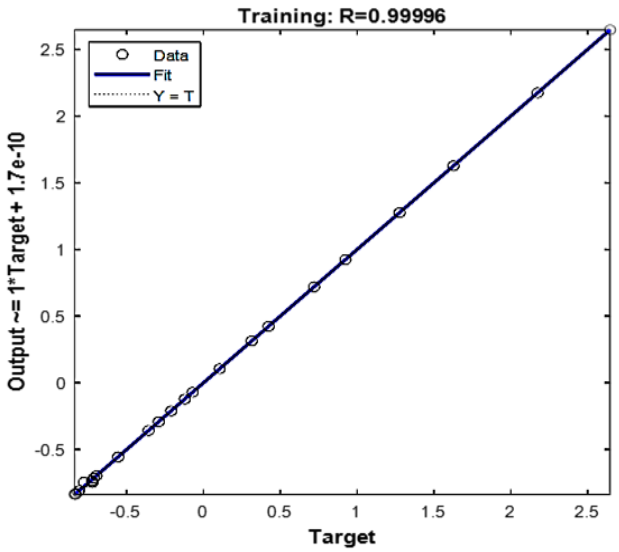

Fig. 3. The ANN model training step compared to the actual field data

Furthermore, the comparison of the Auto-Correlation Function ACF and the Partially Auto-Correlation Function PACF for the calculated differences between the experimental and the predicted model`s data is illustrated in Figure 4. The proposed model is relatively close to the field data and the predictable errors have an arbitrary behavior.

Although the statistical comparison between the two approaches; the mathematical model and the ANN model for the thermal hardening process, shows a little upper hand of the ANN (Table 2), the shorter time, easiness, and less need for sophisticated hardware and software with the use of the mathematical modeling, make it preferable for the administrators and the manufacturers.

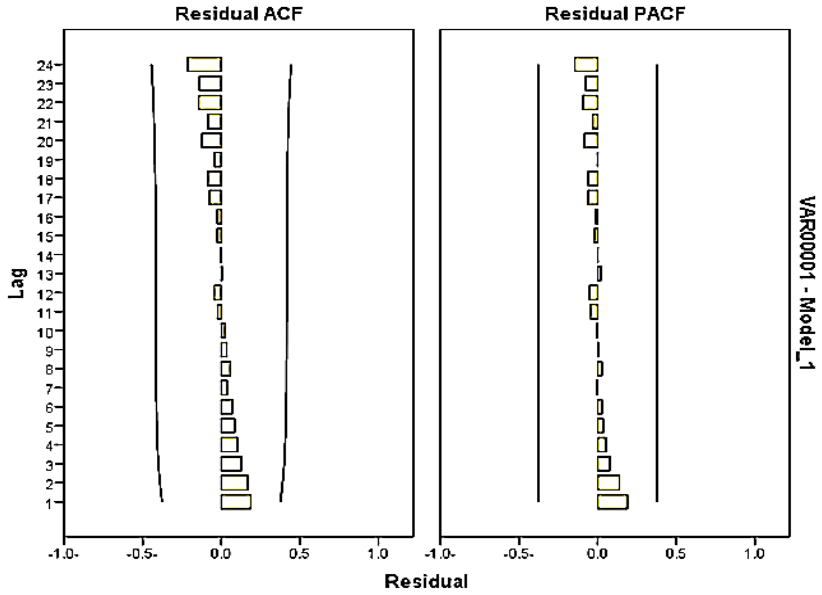

Fig. 4. The residual errors of the ACF and PACF of the ANN predicted model

Table 2. A comparison between the suggested mathematical model and the ANN model

Parameter / Model	Root mean squared error RMSE	R^2
Mathematical model	0.943	0.912
ANN	0.622	0.999

4. CONCLUSIONS

The raise of performance control of industrial projects via the mathematical modeling of the thermal hardening process that highly affects the durability of the exterior surfaces of the in-process tools are demonstrated and analyzed via the equivalent thermal approach in which the material's thermal resistance of exterior layers of the functioned tools are exemplified by the reciprocal value of nodes thermal conductivity and considering the material`s exterior layer and the system units of work tool's heat dissipation, with the attentiveness that the number of the separating parts in the equivalent heat pattern or thermal resistance depends on the selection of heat dissipation system according to the procedure of the setting of the cooling process to be applied on the work tool or the whole production machine. The resulting mathematical model is accompanied by the ANN analysis on the same field data from the Baghdad central complex that includes many big to intermediate workshops, to compare the resulting ANN model with the mathematical one based on precision and the degree of sophistication of application and handling. The first indication from the results of the two approaches is that, although the ANN approach determines very high precision, the mathematical model is not too far from that precision and this in turn accompanied by less complexity and less need for expensive calculating devices/ software make it; the mathematical modeling more preferable. The peak temperature in the location of the contact area of deformation and analogous speed of processing is determined as an important factor for the hardening work tool to select the coating material for the upper layer that progresses to the critical phase of transferal instability.

5. REFERENCES

1. Blankart, C.; Wesselmecking, S.; Krupp, U., (2021). *Influence of Quenching and Partitioning Parameters on Phase Transformations and Mechanical Properties of Medium Manganese Steel for Press-Hardening Application*. Metals, 11, 1879.
2. Bogdan Oancea, Stefan Cristian Ciucu, (2014). *Time series forecasting using neural networks*. Proceedings of the CKS International Conference, arXiv: 1401.1333v1.
3. Charles K., Alexander, Matthew N.O., Sadiku, (2012). *Fundamentals of Electric Circuits.* McGraw-Hill Education
4. Farrahi, G.H. and Sistaninia, M., (2009). *Thermal Analysis of Laser Hardening for Different Moving Patterns*. International Journal of Engineering, Transactions A, 22, 169-180.
5. Hung, T.P., Shi, H.E. and Kuang, J.H. (2018). *Temperature Modeling of AISI 1045 Steel during Surface Hardening Processes*. Materials, 11, 1815. https://doi.org/10.3390/ma11101815.

6. Jose Manuel Dıaz Moreno, Concepcion Garcıa Vazquez, Marıa Teresa Gonzalez Montesinos, Francisco Ortegon Gallego, Giuseppe Viglialoro, (2017). *Steel heat treating: mathematical modelling and numerical simulation of a problem arising in the automotive industry*. Advances in Science, Technology and Engineering Systems Journal, 2(5), 55-62.
7. Makarova S.S., Dement'yeva V.B., Makarova E.V., (2016). *Mathematical Modeling of Cooling High-Temperature Cylindrical Workpieces*. Procedia Engineering, 150, 393-399.
8. Mathioulakis, E., Panaras, G., and Belessiotis, V., (2018). *Artificial neural networks for the performance prediction of heat pump hot water heaters*. Int. J. Sustain. Energy, 37(2), 173–192.
9. Samani, M.K., Ding, X.Z., Khosravian, N., Amin-Ahmadi, B., Yang Yi, Chen, G., Neyts, E.C., Bogaerts, A., Tay, B.K., (2015). *Thermal conductivity of titanium nitride/titanium aluminum nitridemultilayer coatings deposited by lateral rotating cathode arc*. Thin Solid Films, 578, 133-138.
10. Tan, T. and Zhou, H., (2013). *Numerical Solution for a Transient Temperature Distribution on a Finite Domain Due to a Dithering or Rotating Laser Beam*. International Journal of Operations Research and Information Systems, 4, 22-38.
11. Tarchoun, B., El Ouafi, A. and Chebak, A., (2020). *Numerical Investigation of Laser Surface Hardening of AISI 4340 Using 3D FEM Model for Thermal Analysis of Different Laser Scanning Patterns*. Modeling and Numerical Simulation of Material Science, 10, 31-54.
12. Weia, R., Enomotoa, M., Hadianb, R., Zurobb, H.S., and Purdy, G.R., (2013). *Growth of austenite from as-quenched martensite duringintercritical annealing in a Fe–0.1C–3Mn–1.5Si alloy*. Acta Materialia, 61, 697–707.
13. Yuehui Chen, Bo Yang, Jiwen Dong, and Ajith Abraham, (2005). *Time-series forecasting using flexible neural tree model*. Inf. Sci. (Ny), 174(3–4), 219–235.

Received: June 3, 2022 / Accepted: December 15, 2022 / Paper available online: December 20, 2022 © International Journal of Modern Manufacturing Technologies